Int J Biometeorol (1999) 42:146–152

ORIGINAL ARTICLE

Jacques Régnière · Alexei Sharov

Simulating temperature-dependent ecological processes at the sub-continental scale: male gypsy moth flight phenology as an example

Received: 26 May 1998 / Accepted: 6 July 1998

Abstract We simulated male gypsy moth flight phenology for the location of 1371 weather stations east of 100° W longitude and north of 35° N latitude in North America. The output of these simulations, based on average weather conditions from 1961 to 1990, was submitted to two map-interpolation methods: multiple regression and universal kriging. Multiple regression was found to be as accurate as universal kriging and demands less computing power. A map of the date of peak male gypsy moth flight was generated by universal kriging. This map itself constitutes a useful pest-management planning tool; in addition, the map delineates the potential range of the gypsy moth based on its seasonality at the northern edge of its current distribution in eastern North America. The simulation and map-interpolation methods described in this paper thus constitute an interesting approach to the study and monitoring of the ecological impacts of climate change and shifts in land-use patterns at the sub-continental level.

Key words Landscape ecology · Area-wide management · Modelling · Interpolation · Kriging · Regression · Climate change

Introduction

There is growing scientific interest in variation of the phenology of the landscape in response to climatic factors, especially temperature and moisture. Plants, microorganisms and the vast majority of animals that make up the ecosystems are poikilotherms, and the rates of their biological reactions depend on temperature and moisture. Climatic fluctuations can lead to spatial and temporal variations in the development of, and synchrony between, different groups of organisms. Such variation, in turn, generates landscape-level spatial and temporal patterns in the abundance and quality of organisms. A better understanding of the underlying causes of such spatial patterns may clarify the influence of temperature-dependent phenomena on the outcome of ecological processes such as seasonality, migration and population dynamics (Coulson et al. 1993; Pulliam et al. 1992; With 1994). This knowledge is central to our ability to understand ecosystems and to predict the impact of natural and man-made changes in the climatic environment (Duffy et al. 1994; de Groot et al. 1995).

The ability to predict the development of organisms accurately in heterogeneous landscapes is also a critical element of area-wide pest management (Bell and Hardee 1994; Gressel et al. 1996; Lamp and Zhao 1993), which is a spatial extension of the Integrated Pest Management (IPM) concepts developed in the 1970s (Huffaker 1980; Ruesink 1976). IPM was motivated partly by a need to reduce the use of chemical pesticides in the management of agricultural crops and forests. One of the cornerstones of IPM is precise delivery of pesticides to enhance efficacy, reduce side-effects and decrease the need for repeated applications. This remains true in the context of area-wide pest management. In addition, demand for timing accuracy in conjunction with biological control methods, especially microorganisms, and other pest management tools such as semiochemicals (e.g. pheromones, allomones) is on the increase. The way that many of these products work is intricately linked to the phenological state and behaviour of the target organisms, which are often susceptible to these products for only a short period in their life cycle.

Due to the importance of timing and synchrony in ecology and pest management, considerable attention has been focused on the development of phenology models. Much less effort has been devoted to the application of these models to generating area-wide forecasts over large, heterogeneous landscapes. Régnière (1996) designed a generalized approach to the use of temperature-driven simulation models in area-wide pest management.

Prepared in conjunction with a presentation made at the ISB Phenology Symposium, Boston MA, 26–27 March 1998

J. Régnière (✉)
Natural Resources Canada, Canadian Forest Service, Laurentian Forestry Centre, PO Box 3800, Sainte-Foy, Quebec, Canada G1V 4C7

A. Sharov
Department of Entomology, Virginia Polytechnic Institute, Blacksburg, VA 24060, USA

This approach was incorporated into a system called BioSIM (Régnière and Logan 1996; Régnière et al. 1995a). In this approach, some arbitrary feature of model output (e.g. the date of occurrence of a specific developmental stage) is related, by multiple regression, to the location, elevation, slope and aspect of a set of target sites distributed over the area of interest. Temperature input for the simulations is assembled from a set of nearby weather stations, after adjustment for differences in elevation, latitude and exposure to sunlight, and taking into account major maritime influences on thermal gradients. The resulting regression model, called a target function by Schaub et al. (1995), is then used to transform algebraically a digital elevation model (DEM) of the area into a new geo-referenced coverage which Régnière (1996) called a Target Event Map (TEM). The spatial patterns in this TEM can then be analysed or incorporated into decision-making processes. This approach is not limited to timing issues, as any feature derived from the output of temperature-driven simulation models can be the object of such analysis. In addition, BioSIM has been modified to simulate precipitation as well as air temperature. Thus, the outcome of a wide variety of temperature- and moisture-driven ecological phenomena can be modelled and mapped using BioSIM.

BioSIM was initially developed and tested for scales of 1–1000 km^2 (Régnière et al. 1995b). However, the same approach can conceivably be applied to much larger areas (>10,000 km^2). This scale would be useful in the prediction and interpretation of broad spatio-temporal patterns in temperature- and moisture-driven phenomena in response to global change (climate or land-use). However, it is not clear whether the multiple regression approach to map generation proposed by Régnière (1996) is well suited to such a scale. Geographical variation in the weather can be affected by major geologicial features that can lead to complex spatial patterns and autocorrelation in model outputs, making multiple regression inappropriate.

In this paper, we compare multiple regression and universal kriging as methods for mapping phenology model output at the sub-continental scale. Kriging is a commonly used geostatistical interpolation method based on spatial autocorrelation (Issaks and Srivastava 1989). As a case study, this comparison is made for a map of the expected date of the male gypsy moth, *Lymantria dispar* (Lepidoptera: Lymantriidae), peak flight over northeastern North America. We also discuss further generalization of the target-function approach to take into account an arbitrary number of continuous and categorical variables in projecting simulation model outputs to the landscape level.

Methods

As a case study, we used a temperature-driven model of gypsy moth development described and validated by Régnière and Sharov (1998). This model was assembled from a collection of sub-models describing the developmental response to temperature of post-diapause eggs (Johnson et al. 1983), the first four larval stages (Logan et al. 1991), and the subsequent life stages until moth emergence (Sheehan 1992). Daily minimum and maximum air temperature are used as inputs for the model, which then yields the daily number of living adult moths of both sexes.

We obtained a digital elevation model (DEM) for eastern North America from World Wide Web site http://edcwww.cr.usgs.gov/landdaac/gtopo30/gtopo30.html. This DEM was cropped to the south at 35° N, to the north at 52° N latitude and to the west at 100° W longitude. Its resolution was reduced to 2 arc min (approximately 4 km) by averaging neighbouring elevations at an original resolution of 30 arc s (approximately 1 km). Because of the low resolution of this DEM, there was no point in including slope and aspect in this study.

Historical air temperature data for the US portion of the map were downloaded from the US National Climatic Data Center's Historical Climatology Network (USHCN) (World Wide Web site ftp:/ftp.ncdc.noaa.gov/pub/data/ushcn). These data, contained in files URBAN.MIN and URBAN.MAX, consist of monthly average minimum and maximum temperatures, by year, corrected for biases due to urban development. The latitude, longitude and elevation of the weather stations in this database were obtained from file STATION.INVENTORY. From these monthly means, normals for the latest standard normal-generating period (SNGP, 1961–1990) were calculated for the creation of a database of normals for BioSIM. These normals are mean monthly average minimum, mean and maximum air temperatures as well as extreme minimum and maximum temperatures. BioSIM uses extremes to generate stochastic daily temperature data (Régnière and Bolstad 1994). Extremes were estimated for each station from the deviation between the overall monthly mean minimum or maximum ($M_{\min}$, $M_{\max}$) and the lowest monthly mean minimum or maximum recorded over the SNGP ($L_{\min}$, $L_{\max}$):

$$\begin{aligned} X_{\min} &= M_{\min} - 7.5(L_{\min} - M_{\min}) \\ X_{\max} &= M_{\max} + 7.5(L_{\max} - M_{\max}) \end{aligned} \quad (1)$$

The factor of 7.5 produced realistic daily temperature ranges compared with actual ranges. Air temperature data for the Canadian portion of the map were obtained from the Canadian Monthly Climate Data and 1961–1990 Normals and Monthly Averages 1993 CD-ROM (Climate Information Branch, Environment Canada, Ottawa, Ontario, Canada). These data were used without modification.

Due to the stochastic nature of the air temperature regime assembly algorithm in BioSIM (see Régnière and Bolstad 1994), five replicated simulations were run for each of the 1371 points corresponding to the weather stations in our database located in the area covered by the DEM (Fig. 1). A table consisting of latitude N, longitude W, elevation E and date of peak moth abundance D (averaged over replicates) was compiled from model outputs. Dates in this table were limited to Julian Day 273 (3rd week of September). We used this date as a realistic limit beyond which the gypsy moth would be unable to complete its life cycle and thus would not persist (see Régnière and Sharov 1998). This table is hereafter referred to as the dataset.

As a first step in the comparison of kriging and multiple regression as interpolation methods, three universal kriging detrending models were fitted to the model output table:

$$D = a + \alpha E \quad (2)$$

$$D = a + \alpha E + bN + cW \quad (3)$$

$$D = a + \alpha E + bN + cW + dN^2 + eW^2 + fNW \quad (4)$$

where the term in E is an external drift term, terms in N and W are trend terms and α, a–f are parameters. We first constructed an isotropic semi-variogram from the residuals of each detrending model, using 50 lags of 7 km (with a search tolerance of ±3.5 km) with module GAM2V of the GSLIB library (Deutsch and Journel 1992). Each of the three resulting semi-variograms was fitted with three models: spherical, exponential and Gaussian

$$\hat{\gamma}_h = \begin{cases} c_0 + c_1\left[1.5h/a - 0.5(h/a)^3\right] & \text{if } h < a \\ c_0 + c_1 & \text{otherwise} \end{cases} \quad (5)$$

$$\hat{\gamma}_h = c_0 + c_1(1 - e^{-h/a}) \quad (6)$$

$$\hat{\gamma}_h = c_0 + c_1[1 - e^{-(h/a)^2}] \quad (7)$$

where $\hat{\gamma}_h$ is the semi-variance of pairs of points located a distance h apart, c_0 is the nugget, c_1 is the semi-variance contribution (sill–nugget, see Isaaks and Srivastava 1989) and a is the semi-variogram range.

Parameters for Eqs. 5–7 were estimated using Powell's (1965) iterative non-linear regression algorithm by weighted least-squares rather than by ordinary least-squares, as suggested by Cressie (1993), to reduce potential variance estimate bias. The algorithm minimized the sum of weighted squared residuals given by:

$$RSS = \sum_{j=1}^{k} \frac{N(h_j)}{\gamma(h_j)^2} \left[\hat{\gamma}(h_j) - \gamma(h_j)\right]^2 \quad (8)$$

where $N(h_i)$ is the number of distinct pairs of points contributing to the estimate $\gamma(h_j)$ of semi-variance at lag h_j, and $\hat{\gamma}(h_j)$ is the expected semi-variance. The best semi-variogram model was selected on the basis of goodness of fit as well as graphical examination, placing particular emphasis on fit at or near the nugget.

The interpolation multiple regression model used was a 26-term second-degree polynomial in N, N^2, W, W^2, E, E^2, NW, WE, NE, NW^2, EW^2 WN^2, WE^2, EN^2, NE^2, WNE, N^2W^2, W^2E^2, N^2E^2, NEW^2, WEN^2, WNE^2, EN^2W^2, NW^2E^2, WN^2E^2, WN^2E^2 and $W^2E^2N^2$. The comparison of universal kriging and multiple regression was done using a two-stage cross-validation process. The dataset was divided into two independent halves. In each stage of cross-validation, one half of the data was used to estimate a new set of detrending and semi-variogram or multiple regression parameters, while the other half served to compute the cross-validation coefficient of determination:

$$R^2 = 1 - \frac{\sum_{i=1}^{n} (D_i - \hat{D}_i)^2}{\sum_{i=1}^{n} (D_i - \overline{D}_i)^2} \quad (9)$$

Fig. 1 Elevation map of northeastern North America showing the location of the 1371 weather stations used as simulation points

where D_i is the observed date at location i (and n is half the number of locations in the whole dataset), $\overline{D}_i$ is the average observed date in the half data set, and $\hat{D}_i$ is the date predicted either by the multiple regression model or by the universal kriging algorithm. Universal kriging was done with module XVKT3D of the GSLIB library (Deutsch and Journel 1992), using a search radius of 500 km and estimation based on the 10–20 nearest sample points. Average bias β was also calculated:

$$\beta = \frac{\sum_{i=1}^{n} (D_i - \hat{D}_i)}{n} \quad (10)$$

Kriging cross-validation results obtained with detrending models 2, 3 and 4 were compared with the results obtained with the 26-term multiple regression model. Finally, a map of the expected date of peak male gypsy moth flight was prepared using KTB3D of the GSLIB library (Deutsch and Journel 1992) and our DEM as the underlying drift map.

Results

Weather stations in our database were not evenly distributed over the geographical area covered by our DEM. Much of this unevenness was due to the Canadian portion of the database (Fig. 1). Stations are quite scarce in northern Ontario and along the north shore of the St. Lawrence estuary in Quebec. There was also a high concentration of stations in the St. Lawrence valley in southern Quebec around Montreal. We judged that, given the large number of stations, this somewhat uneven distribution would not unduly affect the analyses, but results obtained for the northernmost latitude must be interpreted with caution.

The 26-term multiple regression model relating the date of peak male gypsy moth flight D to latitude, longi-

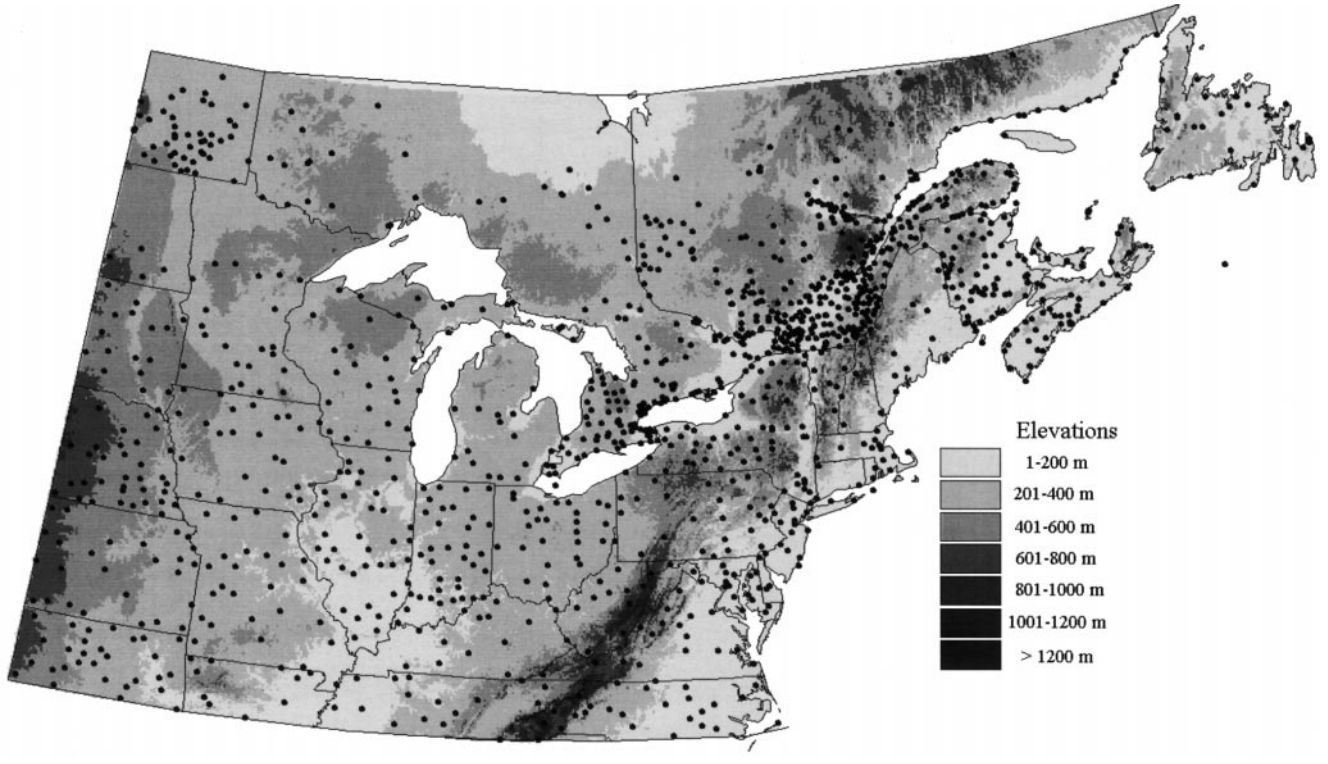

Table 1 Multiple regression analysis of the predicted date of peak male gypsy moth flight in eastern North America. (*N* Latitude, *W* longitude, *E* elevation)

Term	*df*	Sequential SS	Adjusted SS	*F*	*P*
W	1	435,903	2,149	39.2	0.001
N	1	767,275	31,369	572.0	0.001
E	1	47,964	6,925	126.3	0.001
W^2	1	9,030	1,866	34.0	0.001
WN	1	6,798	489	8.9	0.003
WE	1	129	106	1.9	0.165
N^2	1	104	3,009	54.9	0.001
NE	1	369	522	9.5	0.002
E^2	1	2,611	1,402	25.7	0.001
W^2N	1	7,576	1,119	20.4	0.001
W^2E	1	10,888	8,615	157.1	0.001
WN^2	1	8,870	44	0.8	0.370
WNE	1	387	234	4.3	0.039
WE^2	1	1,257	263	4.8	0.029
N^2E	1	4,238	626	11.4	0.001
NE^2	1	624	564	10.3	0.001
W^2N^2	1	1,591	2,696	49.2	0.001
W^2NE	1	2	464	8.5	0.004
W^2E^2	1	2,279	3,325	60.6	0.001
WN^2E	1	4,623	430	7.8	0.005
WNE^2	1	501	347	6.3	0.012
N^2E^2	1	294	75	1.4	0.242
W^2N^2E	1	394	1,214	22.1	0.01
W^2NE^2	1	269	216	3.9	0.048
WN^2E^2	1	217	9	0.2	0.689
$W^2N^2E^2$	1	1,032	1,032	18.8	0.001
Error	1345	73,764			
Total	1371	1,388,985			

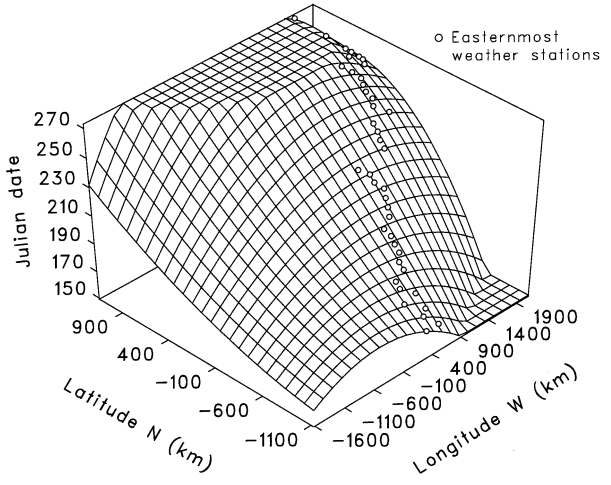

Fig. 2 Multiple regression describing the influence of latitude and longitude on the date of peak male gypsy moth flight in northeastern North America. *Open circles* are a subset of sample simulation points outlining the eastern edge of the continent. Surface calculated for average elevation. The biologically realistic limit to the date of flight was set to Julian day 273 (end of the 3rd week of September)

tude and elevation provided a good overall fit (R^2=0.947; Table 1). Latitude (*N*, N^2) explained 55.2% of total variation in *D*, while longitude (*W*, W^2) and elevation (*E*, E^2) explained 32.0% and 3.6%, respectively. All other terms combined explained an additional 3.9% of variation in

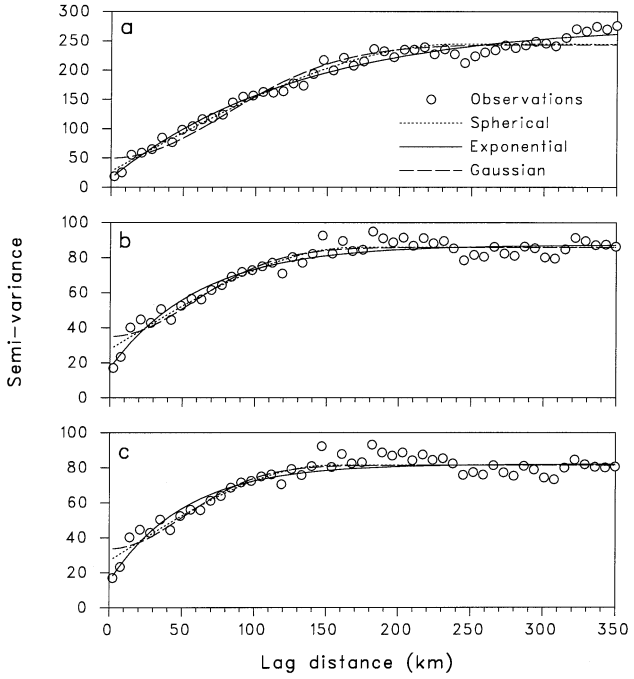

Fig. 3a–c Isotropic semi-variograms calculated on dates of peak male gypsy moth flight using different detrending models. **a** Eq. 2; **b** Eq. 3; **c** Eq. 4. *Lines* are semi-variogram models: *dotted* is Eq. 5, *solid* is Eq. 6, *dashed* is Eq. 7

D, and most were highly significant (P<0.01). The curvilinear and interaction terms produced a relatively complex response surface (Fig. 2). There was an overall south to north gradient in moth flight date averaging 4.6 days per 100 km north. This gradient was least pronounced at the western edge of the map (3 days per 100 km north), and most pronounced on the eastern seaboard (7 days per 100 km north). There was also a pronounced increase in the dates of moth flight from west to east, averaging 1.7 days delay per 100 km east. This longitudinal gradient was most pronounced in the northern section of the study area. The influence of elevation *E* also varied with latitude and longitude. It averaged 4.6 days per 100 m elevation, and was most pronounced to the west and north. Several simulation points at the northeastern limit of our geographical span were subject to the imposed constraint that D<274. However, we verified that removal of these points from the analysis did not change the regression results.

Without detrending the date of peak flight other than for external drift due to elevation (Eq. 2), semi-variance failed to converge and exceeded a value of 250 at lags of up to 350 km (Fig. 3a). Detrending with Eq. 3 reduced maximum semi-variance to around 85, and a clear sill was reached at lag distances of 125–150 km (Fig. 3b). A more complex detrending model (Eq. 4) presented no additional advantage (sill=80, range=125 km; Fig. 3c). We have found that, in general, simpler detrending models produce better universal kriging results than more complex models. The spherical model (Eq. 5) had the best-fit R^2 to all semi-variograms (Table 2). However, the expo-

Table 2 Semi-variogram non-linear regression analysis goodness-of-fit (R^2) values

Detrending model	Semi-variogram model		
	Spherical – Eq. 5	Exponential – Eq. 6	Gaussian: Eq. 7
Eq. 2	0.966	0.978	0.957
Eq. 3	0.942	0.933	0.924
Eq. 4	0.918	0.903	0.900

Table 3 Cross-validation result summary (average values of two-step process)

	Kriging			Multiple regression
	Eq. 2	Eq. 3	Eq. 4	
Mean bias	0.14	0.11	0.04	–0.05
Mean % bias	0.06	0.05	0.02	0.02
R^2	0.956	0.959	0.944	0.940

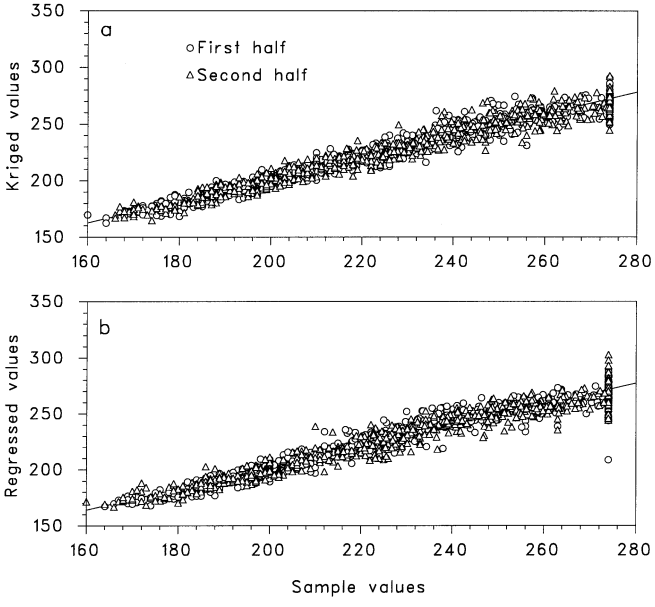

Fig. 4a, b Relationships between sampled and estimated values of male gypsy moth peak flight dates obtained by two-stage cross validation. **a** By universal kriging; **b** by multiple regression. (*Circles* Stage one of cross-validation, *triangles* stage two)

nential model (Eq. 6) produced a more realistic estimate of the nugget effect (Fig. 3), and was selected for cross-validation and kriging despite its slightly lower regression R^2.

The multiple regression interpolation method (using Eq. 4) had an average cross-validation R^2 of 0.941, with a prediction bias of 0.02% (Table 3). Kriging cross-validation results were only slightly better, with R^2 ranging from 0.944 to 0.959. Prediction bias was very small in all cases, never exceeding 0.1% of sample values. The best cross-validation fit was obtained with Eq. 3 as a detrending model, but results were virtually identical to

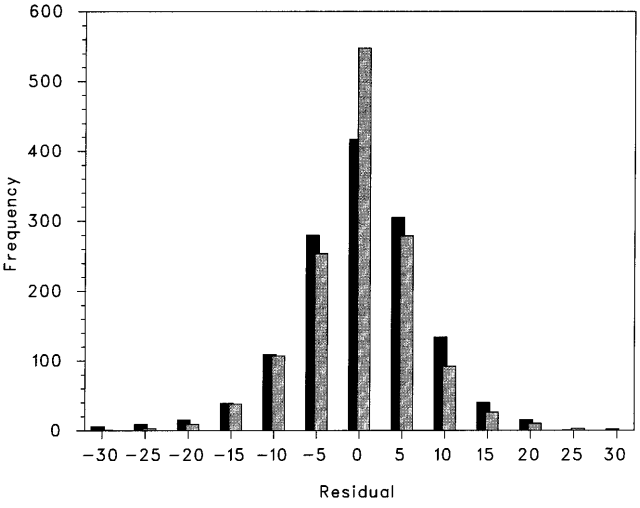

Fig. 5 Frequency distributions of residuals (difference between interpolated and sample values) of the cross-validations. (*Pale bars* Universal kriging, *dark bars* multiple regression)

those obtained with Eq. 2 where there is actually no detrending and only elevation is used as an external drift variable.

Cross-validation prediction using kriging or regression as interpolation methods corresponded closely to sample values, and there was no deviation from the line of unity in any portion of the range of observed values (Fig. 4). The frequency distributions of the cross-validation residuals (predicted–observed) were very similar between the two interpolation methods (Fig. 5). The standard deviation of the residuals was 7.6 and 6.5 days for the multiple regression and kriging cross-validations, respectively. The corresponding average absolute residual values were 5.7 and 4.7 days. Thus, the precision of interpolation by universal kriging was only marginally superior to that of multiple regression.

Universal kriging, using Eq. 3 as the detrending model and Eq. 6 as the semi-variogram model, generated the map of gypsy moth peak flight period in Fig. 6. This map can be used to plan the deployment and retrieval of pheromone traps for monitoring gypsy moth populations, or the application of pheromones for mating disruption purposes. An electronic version of this map can be obtained at WWW site http://www.gypsymoth.ento.vt.edu.

Discussion and conclusions

Universal kriging and multiple regression proved to be nearly equally precise in interpolating the output of our temperature-driven simulation model, as determined by cross-validation. However, kriging required more computing time than did regression analysis. The regression procedure initially proposed for the generation of TEMs with BioSIM (Régnière 1996) therefore seems applicable to maps at the sub-continental scale. Spatial autocorrelation in simulation model outputs at this scale seems to be

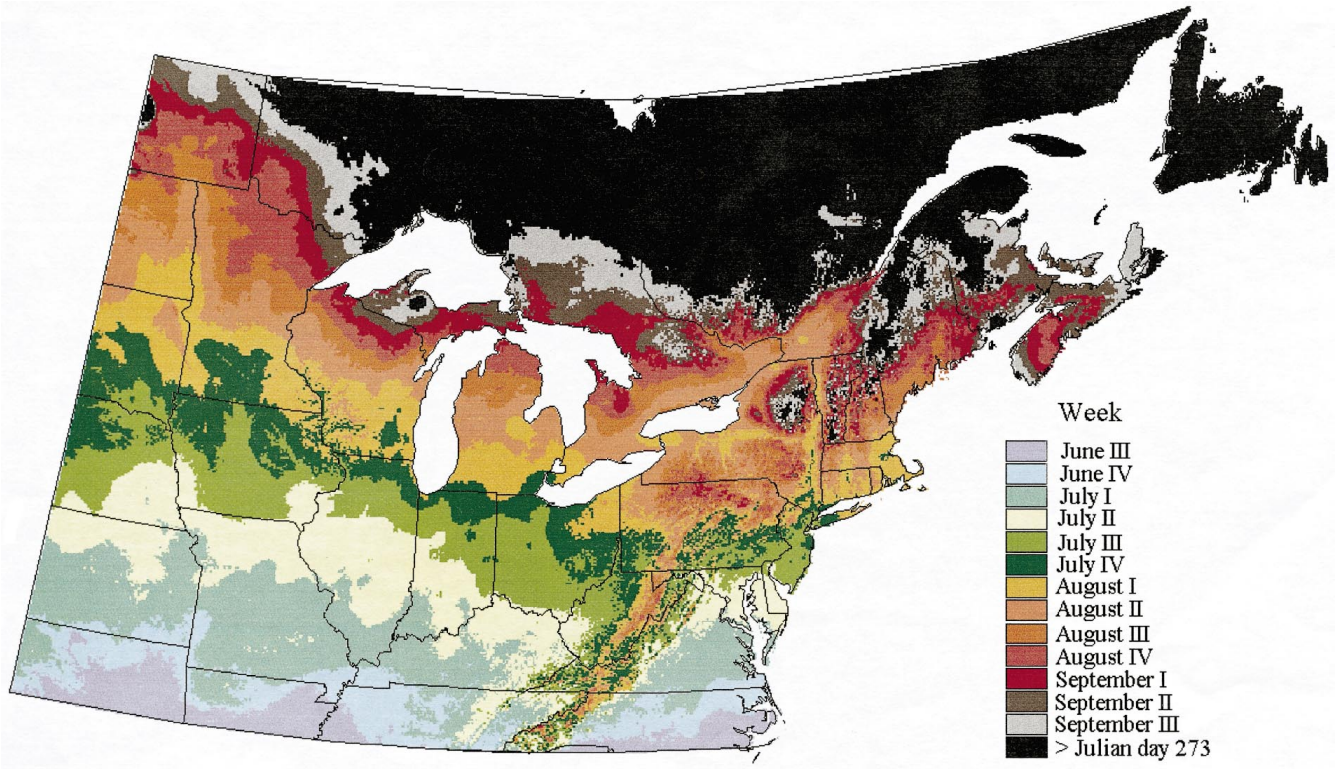

Fig. 6 Kriged map of the expected date of peak gypsy moth male flight over northeastern North America. Note the areas where the simulation model predicts non-persistent seasonality (*darkest areas*)

mostly explained (and removed) by the regression model, eliminating bias in interpolated values. This may be due to the relatively simple physical processes that determine the distribution of air temperature at that scale. Universal kriging (or some other interpolation method based on regional estimation) offers an alternative in cases where simple polynomial terms cannot mimic more complex response surfaces, or at larger scales where physical factors associated with latitude, longitude and elevation may not be the dominant causes of the observed temperature patterns.

The non-linearity captured by the 26-term multiple regression model used to describe the spatial patterns in the data of peak male gypsy moth flight were slight, but resulted in a rather complex response surface (Fig. 2). Much of this complexity probably resulted from the pronounced maritime influences at the eastern edge of the continent and broad variation in water temperature. Because of such non-linearity, the multiple regression method should be used very carefully in extrapolation beyond the observed range of independent variables (polynomials are notoriously poor for extrapolation). In the present study, there was little extrapolation except perhaps at the northern edge of the map. However, the simulation model predicted non-persistent gypsy moth seasonality at much lower latitudes.

Phenology maps at the sub-continental scale can be used not only to help plan the deployment of pest-management resources, but also to study the nature and ecological consequences of seasonality over large areas in response to changes in climate and land-use. In our example, the current geographical distribution of the gypsy moth, especially at its northern edge, is undoubtedly in large part determined by climatic limitations related to seasonality (Fig. 6). Various global warming scenarios could be applied to long-term average temperatures and the consequences in terms of range expansion for this and other insect species could be mapped by the methods proposed here. Of course, several factors in addition to seasonality are important in determining the range and abundance of organisms. For herbivores such as the gypsy moth, vegetation patterns are also critical. Other geographically distributed variables such as soils, moisture, the abundance of food sources, competitors or predators as well as their synchrony with each other can be important determinants. Perhaps the greatest advantage of multiple regression (and its generalization into variance-covariance analysis: general linear models algorithms) is that it can be used to generate spatial interpolations for the output of models driven by an arbitrary number of geographically distributed variables, be they continuous (e.g. moisture, planting date) or categorical (e.g. crop species). The spatial patterns generated by such multivariate interpolations of simulation model outputs can constitute the basis for comparison with observations and the prediction of consequences of global change on seasonality.

Acknowledgements We gratefully acknowledge Manon Gignac for her help in preparing the maps.

References

Bell MR, Hardee DD (1994) Early season application of a baculovirus for area-wide management of *Heliothis/Helicoverpa* (Lepidoptera: Noctuidae): 1992 field trial. J Entomol Sci 29:192–200

Coulson RN, Fitzgerald JW, Saunders MC, Oliviera FL (1993) Spatial analysis and integrated pest management in a landscape ecological context. US Forestry Service General Technical Report NE-175:93–99

Cressie NAC (1993) Statistics for spatial data, revised edition. Wiley, New York

Deutsch CV, Journel AG (1992) GSLIB geostatistical software library and user's guide. Oxford University Press, New York

Duffy DC, Clark DD, Campbell SR, Gurney S, Perello R, Simon N (1994) Landscape patterns of abundance of *Ixodes scapularis* (Acari: Ixodiidae) on Shelter Island, New York. J Med Entomol 31:875–879

Gressel J, Gardner SW, Angel M (1996) Prevention *versus* remediation in resistance management. In: Molecular genetics and evolution in pesticide resistance. American Chemical Society, Washington, DC, pp 69–186

de Groot RS, Ketner P, Ovaa AH (1995) Selection of bio-indicators to assess the possible landscape ecological effects of climate change. Stud Environ Sci 65B:757–762

Huffaker CB (1980) New technology of pest control. Wiley, New York

Isaaks EH, Srivastava RM (1989) An introduction to applied geostatistics. Oxford University Press, New York

Johnson PC, Mason DP, Radke SL, Tracewski KT (1983) Gypsy moth, *Lymantria dispar* (L.) (Lepidoptera: Lymantriidae), egg eclosion: degree-day accumulation. Environ Entomol 12:929–932

Lamp WO, Zhao L (1993) Prediction and manipulation of movement of polyphagous, highly mobile pests. J Agric Entomol 10:267–281

Logan JA, Casagrande RA, Liebhold AM (1991) Modeling environment for simulation of gypsy moth (Lepidoptera: Lymantriidae) larval phenology. Environ Entomol 20:1516–1525

Powell MJD (1965) A method for minimizing a sum of squares of non linear functions without calculating derivatives. Comput J 7:303–307

Pulliam HR, Dunning JB, Liu JG (1992) Population dynamics in complex landscapes: a case study. Ecol Appl 2:165–177

Régnière J (1996) Generalized approach to landscape-wide seasonal forecasting with temperature-driven simulation models. Environ Entomol 25:869–881

Régnière J, Bolstad P (1994) Statistical simulation of daily air temperature patterns in eastern North America to forecast seasonal events in pest management. Environ Entomol 23: 1368–1380

Régnière J, Logan JA (1996) Landscape-wide projection of temperature-driven processes for seasonal pest management decision support: a generalized approach. In: Decision support systems for forest pest management. Proceedings of a workshop at Entomological Society of Canada Annual Meeting, Victoria, BC, 14–19 October, 1995. Canadian Forest Service and B.C. Forestry Research and Development Agreement Report 260, pp 43–55

Régnière J, Sharov A (1998) Phenology of *Lymantria dispar* (Lepidoptera: Lymantriidae), male flight and the effect of moth dispersal in heterogeneous landscapes. Int J Biometeorol 41:161–168

Régnière J, Cooke B, Bergeron V (1995a) BioSIM: a computer-based decision support tool for seasonal planning of pest management activities. User's manual. Canadian Forest Service Information Report LAU-X-116

Régnière J, Lavigne D, Dickison R, Staples A (1995b) Performance analysis of BioSIM, a seasonal pest management planning tool, in New Brunswick in 1992 and 1993. Canadian Forest Service Information Report LAU-X-115

Ruesink WG (1976) Status of the systems approach to pest management. Annu Rev Entomol 21:27–44

Schaub LP, Ravlin FW, Gray DR, Logan JA (1995) Landscape framework to predict phenological events for gypsy moth (Lepidoptera: Lymantriidae) management programs. Environ Entomol 24:10–18

Sheehan KA (1992) User's Guide for GYMPHEN: GYpsy Moth PHENology model. US Forestry Service General Technical Report NE-158

With KA (1994) Ontogenetic shifts in how grasshoppers interact with landscape structure: an analysis of movement patterns. Funct Ecol 8:477–485